Glycolysis is independent of oxygenation state in stimulated human skeletal muscle *in vivo*

Kevin E. Conley, Martin J. Kushmerick and Sharon A. Jubrias

Departments of Radiology, Physiology and Biophysics, and Bioengineering, University of Washington Medical Center, Seattle, WA 98195-7115, USA

(Received 30 October 1997; accepted after revision 15 July 1998)

1. We tested the hypothesis that the cytoplasmic control mechanism for glycolysis is affected by the presence of oxygen during exercise. We used a comparison of maximal twitch stimulation under ischaemic and intact circulation in human wrist flexor and ankle dorsiflexor muscles. ^{31}P magnetic resonance spectroscopy followed the phosphocreatine (PCr), P_i and pH dynamics at 6–9 s intervals. Glycolytic PCr synthesis was determined during stimulation from pH and tissue buffer capacity, as well as the oxidative phosphorylation rate.

2. Ischaemic *vs.* aerobic stimulation resulted in similar glycolytic fluxes in the two muscles. The onset of glycolysis occured after fifty to seventy stimulations and the extent of glycolytic PCr synthesis was directly proportional to the number of stimulations thereafter.

3. Two-fold differences in the putative feedback regulators of glycolysis, [P_i] and [ADP], were found between aerobic and ischaemic stimulation. The similar glycolytic fluxes in the face of these differences in metabolite levels eliminates feedback as a control mechanism in glycolysis.

4. These results demonstrate that glycolytic flux is independent of oxygenation state and metabolic feedback, but proportional to muscle activation. These results show a key role for muscle stimulation in the activation and maintenance of glycolysis. Further, this glycolytic control mechanism is independent of the feedback control mechanism that governs oxidative phosphorylation.

Glycolysis is commonly described as an anaerobic process providing ATP in the absence of oxidative phosphorylation. However, glycolytic flux in anoxic resting muscle is typically low and often does not generate sufficient ATP synthesis to meet ATP demands (Blei *et al.* 1993; Yamada *et al.* 1993). In contrast, far higher rates of glycolysis are found in aerobic muscle during exercise than in anaerobic muscles at rest. This high flux provides between 50 and 100% of the substrate needed for oxidative phosphorylation in exercising muscle of humans (Brooks & Mercier 1994; Connett & Sahlin 1996). Clearly, glycolysis is not simply an anaerobic process and the mechanisms responsible for elevating flux under resting conditions cannot account for the high glycolytic flux found under aerobic exercising conditions.

Muscle stimulation is a key difference between resting and exercising muscle that is related to the control of glycolysis and may account for the high glycolytic flux during exercise. Glycogenolytic and glycolytic fluxes vary with muscle stimulation rate under ischaemic or anoxic conditions in animal and human studies and are much larger than in unstimulated muscle (Karpatkin *et al.* 1964; Özand & Narahara, 1964; Conley *et al.* 1997). Calcium activation of glycogenolysis is a well-known example of how substrate mobilization is related to muscle activation rate (see Connett & Sahlin, 1996). Similarly, a rate limiting enzyme in glycolysis, phosphofructokinase (PFK), may also undergo a reversible phosphorylation with muscle stimulation which decreases the K_m, increases V_{max} and facilitates binding to cytoskeletal elements (Luther & Lee, 1986). If Ca^{2+} activation governs both glycogenolysis and glycolysis, then glycolytic flux should be proportional to stimulation rate independent of oxygenation state or the rate of oxidative phosphorylation. Such an independent control of glycolysis and oxidative phosphorylation would account for the finding of lactate generation in fully aerobic animal and human muscle (Connett & Sahlin, 1996).

An important barrier to characterizing the mechanisms governing glycolysis has been quantifying flux during exercise. Muscle biopsies are limited in the number of variables measured, the time resolution and the muscles that can be examined. The advent of non-invasive ^{31}P magnetic resonance spectroscopy has overcome many of these limitations (Kemp *et al.* 1994). We have previously shown that ^{31}P spectra contain sufficient information to characterize glycogenolytic and glycolytic flux with high time resolution under ischaemic conditions in human muscle *in vivo* (Conley *et al.* 1997). In this paper, we show how to extract the same information under aerobic exercise conditions in two muscle groups that are typically not biopsied.

The purpose of this study was to test the mechanism of glycolytic control by comparison of glycolytic flux during aerobic and ischaemic stimulation in two muscle groups differing in contractile and oxidative properties. The first muscle group was a set of wrist flexors composed of primarily fast-twitch fibres (Johnson *et al.* 1973) and our measurements were centred over the flexor digitorum superficialis, as previously described (Blei *et al.* 1993; Conley *et al.* 1997). The second muscle group lies in the anterior leg compartment and has predominantly slow-twitch, aerobic fibres (Johnson *et al.* 1973). Our measurements were centred over the tibialis anterior. These experiments allowed us to determine whether muscle activation controls glycolytic flux independent of the oxygen content of the muscle and of oxidative phosphorylation.

METHODS

Subjects

Fourteen subjects (10 male, 4 female) were drawn from a population of normal volunteers (25–59 years old). The wrist flexors were studied in eight subjects and the ankle dorsiflexors in six subjects. Low signal to noise prevented analysis in one wrist flexor subject. None of the subjects were in specific training programmes involving the wrist flexor or ankle dorsiflexor musculature at the time of the study, but all were recreationally active. The experimental protocol was approved by the Human Subjects Office of the University of Washington and voluntary, written informed consent was obtained from each subject prior to their participation.

^{31}P magnetic resonance spectroscopy (MRS) acquisition

The wrist flexor experiments used a 2·0 Tesla General Electric CSI spectrometer with a one-pulse ^{31}P MR acquisition. An inductively coupled 4·5 cm diameter circular surface coil was tuned to the phosphorus frequency (34·6 MHz) and held in a fixed position over the forearm within the magnet by a cradle. The ankle dorsiflexor experiments used a 4·5 × 9·0 cm surface coil tuned to the phosphorus frequency (25·9 MHz) and placed over the anterior compartment of the leg. The subjects lay supine in a GE Signa 1·5 Tesla spectrometer, and the leg and foot were held in a fixed position with a plastic holder.

The B_1 field homogeneity was optimized by off-resonance proton-shimming on the muscle water peak. The unfiltered PCr line width (full width at half-maximal height) was typically 4 Hz (wrist flexor muscles) and 4–8 Hz (ankle dorsiflexor muscles). Each subject had a high resolution control ^{31}P spectrum of the resting muscle taken under conditions of fully relaxed nuclear spins (interpulse delay: 20 s (wrist flexors) and 16 s (ankle dorsiflexors)), using a spectral width of +2000 Hz (wrist flexor muscles) or +1250 Hz (ankle dorsiflexors) and 2048 data points, as previously published (Blei *et al.* 1993; Conley *et al.* 1997). Sequential spectra were then obtained during a stimulation–recovery experiment (see below) under partly saturated conditions (interpulse delay: 1·76 s (wrist flexor) or 1·5 s (ankle dorsiflexors)). The spectrum for each time point consisted of four summed acquisitions taken over 9 s (wrist flexors) or 6 s (ankle dorsiflexors). No attempt was made to gate the signal acquisition to the electrical stimulation. These rapidly acquired spectra typically had a 20 : 1 signal-to-noise ratio for the PCr peak.

Analysis of spectra

The free-induction decays were Fourier-transformed into spectra and analysed as described previously (Blei *et al.* 1993; Conley *et al.* 1997). The area corresponding to each spectral peak was expressed as an absolute concentration using the ATP peak referenced to the level reported for muscle biopsies of the human vastus lateralis ([ATP] = 8·2 mM; total [Cr] = 42 mM; Harris *et al.* 1974). The free ADP level was calculated from the creatine kinase equilibrium (Lawson & Veech, 1979). The chemical shift of the P_i peak relative to PCr (−2·54 p.p.m.) referenced to phosphoric acid (0 p.p.m.) was used to calculate pH (Kushmerick & Meyer, 1985).

Experimental protocol

We activated selected muscles in a uniform manner both spatially and temporally over a region larger than the volume subtended by the surface coil using nerve stimulation, as previously described for the wrist flexors (Blei *et al.* 1993). The muscles of the anterior compartment of the leg (tibialis anterior, extensor digitorum longus and extensor hallucis longus) were activated with transcutaneous electrical stimulation of the common peroneal nerve. A 5 × 10 mm cathode was placed over the nerve just below the head of the fibula, and a 15 × 20 mm anode was placed over the ankle dorsiflexor muscles about 20 mm anterodistal to the cathode. We determined maximal activation of the muscles with the EMG technique used for the wrist flexors.

For the ischaemic experiments, a pressure cuff located over the upper arm or thigh was inflated to 100 Torr above systolic blood pressure prior to stimulation to block blood flow to the muscles. The muscle EMG was unaffected by this ischaemia (Blei *et al.* 1993). The cuff was inflated 6 min (wrist flexors) or 30 s (ankle dorsiflexors) prior to stimulation. We recently reported (Conley *et al.* 1997) that the shorter ischaemic period reduced the discomfort of the experiment but did not significantly affect contractile costs. The cuff remained inflated during the 1 Hz stimulation of the wrist flexors (128 s, 14 spectra) and the 3 Hz stimulation of the ankle dorsiflexors (90 s, 15 spectra). The cuff was released 99 s (11 spectra) after stimulation for the wrist flexors and immediately after stimulation for the ankle dorsiflexors. A period of aerobic recovery was monitored for 612 s (68 spectra, wrist flexors) and 270 s (45 spectra, ankle dorsiflexors).

Calculations

Our goal was to measure carbon substrate flux in glycolysis based on the fate of the glycolytic end-products H^+ and pyruvate. We show below how these end-products are quantified using the dynamics of the P_i and PCr peaks in the ^{31}P spectra during stimulation and recovery. The net PCr synthesis caused by glycogenolysis is stoichiometrically coupled to lactate production via three reactions: ATPase, creatine kinase and lactate dehydrogenase. PCr synthesis and breakdown caused by ATP synthesis and breakdown is coupled to the first two processes. For this reason, we refer to PCr synthesis or splitting as a shortcut to stating ATPase or synthesis coupled to the creatine kinase reaction or to glycogenolysis.

ATP demand and supply. Our analysis of glycolytic flux involves three quantities in the muscle energy balance: (1) ATP use by contraction, (2) ATP synthesis by oxidative phosphorylation and (3) ATP synthesis by glycolysis. The first step of our analysis was to calculate the ATP use by contraction in the presence of oxidative phosphorylation during stimulation to determine whether contractile costs are similar under the two conditions. The ATP synthesis by oxidative phosphorylation was also used in the estimation of pyruvate oxidation under aerobic stimulation conditions. We used this oxidized fraction of glycolytic flux plus H^+ production to define glycolytic ATP synthesis.

Table 1. Glossary of PCr variables

Symbol	Definition
ΔPCr_e	Measured [PCr] change
ΔPCr_i	[PCr] change from rest to first-exercise points
ΔPCr_a	[PCr] change due to oxidative ATP synthesis
ΔPCr_{e-a}	Estimated [PCr] change during stimulation without oxidative ATP synthesis ($= \Delta PCr_e - \Delta PCr_a$)
ΔPCr_c	Contractile [PCr] change
ΔPCr_o	PCr synthesis from glycolytic flux that is oxidized ($= 3/37\ \Delta PCr_a\ k$)
ΔPCr_g	Total glycolytic PCr synthesis ($= (\Delta H^+ 1{\cdot}5) + \Delta PCr_o$)

Separation of the contractile costs from ATP synthesis uses the dynamics of PCr during stimulation and recovery as illustrated in Fig. 1. Figure 1*A* shows the PCr recovery rate resulting from oxidative phosphorylation following stimulation, which is fitted with a monoexponential function to estimate the oxidative phosphorylation rate. This rate was calculated as the difference of the estimated PCr level between two successive time points (ΔPCr_a) divided by the time interval (Δt). The ADP level at this phosphorylation rate was calculated using the creatine kinase reaction and the mean of the metabolite values determined at each time point:

$$[ADP] = [ATP][Cr]([PCr][H^+][K_{eq}])^{-1}, \quad (1)$$

where K_{eq} is the creatine kinase equilibrium constant ($1{\cdot}66 \times 10^9$ M^{-1}). These data permit construction of the phosphorylation rate ($\Delta PCr_a/\Delta t$) *vs.* the [ADP] relationship shown in Fig. 1*B*, which is well fitted using the Hill equation for oxidative phosphorylation (Jeneson *et al.* 1996):

$$\Delta PCr_a/\Delta t = (Max - Min)\left(\frac{([ADP]/[ADP]_{0{\cdot}5})^n}{(1+([ADP]/[ADP]_{0{\cdot}5})^n}\right) + Min, \quad (2)$$

where Max and Min are y-asymptotes of the function, $[ADP]_{0{\cdot}5}$ is the ADP concentration at the half-maximal rate and n is the Hill coefficient. We use the conventional value of 0·03 mM for the $[ADP]_{0{\cdot}5}$ and a n value of 2·2, which is the average value for oxidative phosphorylation *in vivo* and *in vitro* (Jeneson *et al.* 1996). The Max and Min values for each subject were fitted using a least squares fitting routine. Application of this equation to estimate oxidative phosphorylation rate during stimulation assumes that the relationship between [ADP] and rate determined during recovery from exercise also holds during exercise. This assumption is evaluated by comparing the measured contractile cost to that estimated by subtracting the contribution of the estimated oxidative phosphorylation, as described below.

The contribution of oxidative ATP synthesis (ΔPCr_a) to the PCr level during exercise (PCr_e) is subtracted using eqn (2) and yields the PCr level in the absence of oxidative phosphorylation (PCr_{e-a}), as shown in Fig. 1*C*. The initial PCr_{e-a} breakdown provides the measure of ATP cost of contraction (ΔPCr_c), as shown in Fig. 1*D*. This contractile cost is estimated by linear regression of [PCr] *vs.* the number of stimulations starting with the last control spectrum and ending prior to the onset of glycolysis at the peak of pH alkalinization (50–70 stimulations).

Estimation of glycolytic flux

The carbon flux generated by glycolysis is either oxidized by respiration or generates lactate (or alanine) and H^+. Quantifying the H^+ stored in the muscle involves the measured pH and the buffering capacity of the individual muscle. This capacity is composed of two components: the apparent capacity (β_a) and the P_i capacity (β_{P_i}). The initial change in PCr (ΔPCr_i) and alkalinization of pH (ΔpH_i) during the stimulation period provide a means of measuring β_a:

$$\beta_a = \gamma\, \Delta PCr_i/\Delta pH_i, \quad (3)$$

where γ is the proton stoichiometric coefficient of the coupled Lohman reaction, as described previously (Conley *et al.* 1997; Kushmerick, 1997). The contribution of P_i to β_a during the

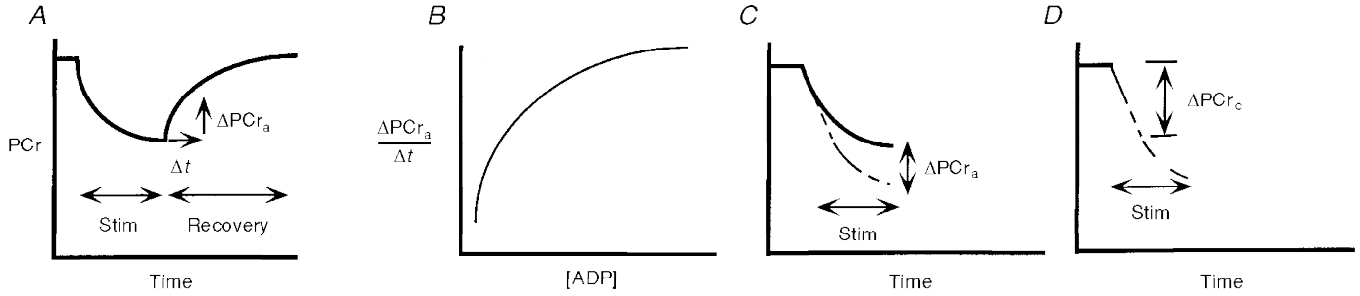

Figure 1. Scheme depicting the method for quantifying oxidative phosphorylation and estimating contractile costs during aerobic stimulation

A, PCr dynamics during recovery following stimulation measures phosphorylation rate ($\Delta PCr_a/\Delta t$). *B*, phosphorylation rate *vs.* [ADP]. *C*, subtraction of PCr synthesis from that measured (PCr_e) to yield PCr level in absence of aerobic synthesis (PCr_{e-a}). *D*, the initial slope of PCr_{e-a} *vs.* time measures contractile cost (ΔPCr_c).

alkalinization period of stimulation is determined based on the dissociation constant of the buffer (K'_a) by the standard formula:

$$\beta_{P_i} = 2{\cdot}303[H^+]K'_a[P_i]/(K'_a + [H^+])^2, \quad (4)$$

where K'_a is $1{\cdot}58 \times 10^{-7}$ M. This contribution is subtracted from β_a to yield the tissue buffer capacity, β_t, which we assumed is constant over the small range of pH in this experiment. The sum of β_t and β_{P_i} is the buffer capacity of muscle, β_{tot}.

Protons are also consumed during PCr breakdown (ΔPCr_e) via the creatine kinase reaction, which depends on the H^+ stoichiometric coefficient (γ) of the coupled Lohman reaction (Kushmerick, 1997). This H^+ consumption plus that stored in the muscle yields the H^+ generation by glycolysis (ΔH^+), which is calculated directly from the observed spectroscopic data using the change in PCr and pH between successive spectra:

$$\Delta H^+ = \Delta pH_e \beta_{tot} + \gamma \Delta PCr_e. \quad (5)$$

The second fate of carbon flux through glycolysis is oxidization of pyruvate by oxidative phosphorylation (ΔPCr_o). This oxidation is estimated based on three ATP molecules generated by glycolysis of a glucosyl unit out of the thirty-seven ATP molecules generated in oxidation of glycogen to CO_2 and H_2O (assuming that all cytosolic NADH enters the mitochondrion via the glycerol phosphate shuttle rather than the thirty-nine ATP molecules generated if NADH enters via the malate/aspartate shuttle):

$$\Delta PCr_o = 3/37\, \Delta PCr_a\, k, \quad (6)$$

where k is the fraction of oxidative phosphorylation that oxidizes pyruvate. We used a conservative estimate that pyruvate oxidation comprises half the substrate supply to oxidative phosphorylation ($k = 0{\cdot}5$) as measured in human muscle at low exercise levels (see Brooks & Mercier 1994).

PCr synthesis resulting from the carbon flux through glycolysis (ΔPCr_g) is the sum of the synthesis resulting from the flux that generates protons (ΔH^+) and that which is oxidized (ΔPCr_o):

$$\Delta PCr_g = (\Delta H^+ 1{\cdot}5) + \Delta PCr_o, \quad (7)$$

where 1·5 is the net H^+ stoichiometry per ATP molecule in glycolysis.

Statistics

Mean differences between treatment and control conditions are stated at the 0·05 level of significance based on Student's two-tailed, paired t test. Values are given as the mean ± S.E.M. throughout unless stated.

RESULTS

Our goal was to compare glycolytic flux under ischaemic and aerobic stimulation conditions in the wrist flexor and ankle dorsiflexor muscle groups. Achieving this goal involved three stages: (1) quantifying the metabolite and pH levels during stimulation in the two muscle groups, (2) demonstrating that stimulation results in the maximal contractile activation for each nerve stimulation under both conditions in the two muscle groups and (3) quantifying glycolytic flux under ischaemic and aerobic conditions.

Dynamics of metabolite content and pH

The first step of our analysis involved quantifying metabolite levels using spectra of muscle at rest and during experimental conditions. Figure 2 shows representative spectra for the ankle dorsiflexors and we have published

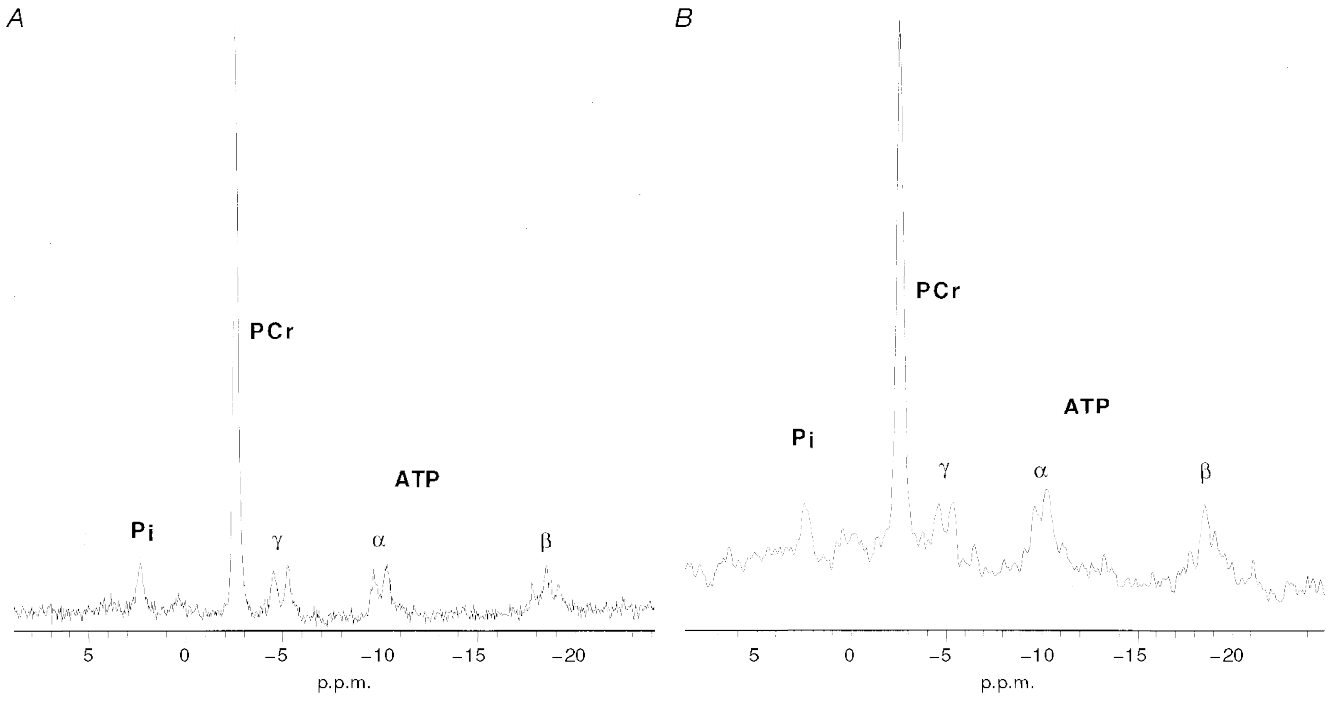

Figure 2. ^{31}P NMR spectra taken during the experiments from the ankle dorsiflexor muscles from a single individual

A, fully relaxed spectrum from 16 acquisitions. *B*, partially saturated spectrum under experimental conditions from 4 acquisitions over 6 s with 4 Hz apodization. The abscissa scale references PCr to a chemical shift of −2·54 p.p.m. relative to phosphoric acid at 0 p.p.m.

similar spectra for the wrist flexors (Blei *et al.* 1993). High-resolution spectra of resting muscle were analysed for each subject to yield the PCr and P_i to ATP ratios. The wrist flexors and ankle dorsiflexors muscle groups have similar PCr/ATP values (3·90 ± 0·21 and 3·98 ± 0·12, respectively) and P_i/ATP (0·53 ± 0·06 and 0·53 ± 0·05, respectively). These ratios were used to calculate absolute concentrations based on the metabolite levels reported for muscle biopsies of the human muscle (Harris *et al.* 1974). Changes in these concentrations throughout the experiment are based on the dynamics of each peak area during stimulation and recovery.

The similar metabolite changes throughout the experiment shown in Fig. 3 for the wrist flexors and ankle dorsiflexors under each condition was achieved by a 3-fold difference in stimulation frequency (1 *vs.* 3 Hz, respectively). Each muscle shows a smaller depletion of PCr and increase in P_i under aerobic as compared with ischaemic conditions. Table 2 shows that the ADP level is also significantly lower under aerobic *vs.* ischaemic stimulation in both muscles. Recovery commences upon the end of stimulation for all conditions except under ischaemia in the wrist flexors. In this experiment alone, ischaemia was held for 99 s after the end of stimulation and then the cuff released. The lack of PCr change during the post-stimulation ischaemic period demonstrates that no significant glycolytic PCr synthesis occurred despite the elevation of metabolite levels, as we and others have previously shown (Wilkie *et al.* 1984; Quistorff *et al.* 1992; Blei *et al.* 1993).

The pH dynamics in Fig. 4 show that the muscles initially alkalinize during the stimulation period under both conditions. The buffer capacity of the cytosol was estimated using the change in pH, PCr and P_i during this period of increasing pH (Adams *et al.* 1990; Conley *et al.* 1997). A decline in pH occured after the peak values and continued throughout stimulation. The final pH was not different from the pre-stimulation level in either muscle group.

Quantifying contractile costs and ATP supply

The second step of our analysis was to determine whether stimulation had the same contractile costs under ischaemia and normoxia. To achieve this goal, we fitted the PCr recovery data to estimate the aerobic ATP synthesis during exercise as outlined in Fig. 1. The recovery phosphorylation rate ($\Delta PCr_a/\Delta t$) and [ADP] were fitted to eqn (2) by estimating the Min and Max coefficients for the Hill equation. The Min coefficients were $-0{\cdot}066 \pm 0{\cdot}030$ and $-0{\cdot}050 \pm 0{\cdot}023$ mM s^{-1} for wrist flexors and ankle

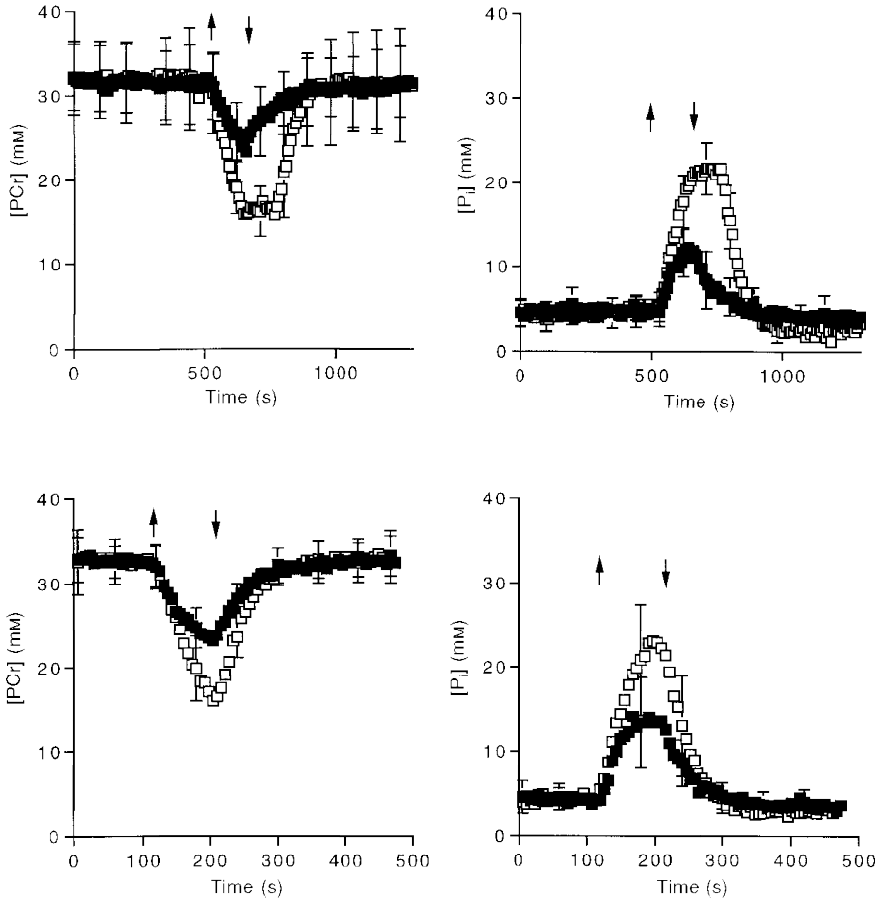

Figure 3. Metabolite levels as a function of time for aerobic (■) and ischaemic (□) stimulation

Values are means ± S.D. Sample size is 8 subjects for the wrist flexor (upper panels) and 6 subjects for the ankle dorsiflexors (lower panels). Arrows indicate the onset and end of stimulation.

Table 2. ADP in muscle at rest and at the end of aerobic and of ischaemic stimulation

	Wrist Flexor		Ankle Dorsiflexor	
	Aerobic	Ischaemic	Aerobic	Ischaemic
[ADP], rest (mM)	0·018 (0·003)	0·017 (0·004)	0·0165 (0·002)	0·015 (0·002)
[ADP], stimulation end (mM)	0·051 (0·005)	0·088 (0·010)	0·047 (0·004)	0·092 (0·014)

Values are means (± S.E.M.).

dorsiflexors, respectively; while the Max coefficients were 0·245 ± 0·065 and 0·330 ± 0·040 mM s^{-1}, respectively. The Max coefficients are lower than measured phosphorylation rates on the same muscle following the ischaemic stimulation (Table 3), which probably results from the lower [ADP] achieved at the end of aerobic *vs.* ischaemic stimulation. Therefore, the Max coefficient does not provide a measure of the maximum mitochondrial oxidative phosphorylation rate. Instead, these coefficients are simply the best fits for the asymptotes of the Hill equation over the [ADP] and $\Delta PCr_a/\Delta t$ measured during recovery from aerobic stimulation. We used eqn (2) to estimate aerobic ATP synthesis (ΔPCr_a) during exercise, which was subtracted from measured PCr (PCr_e) to yield the PCr level in the absence of aerobic ATP synthesis (PCr_{e-a}), as outlined in Fig. 1. The change in PCr_{e-a} (aerobic stimulation) or PCr_e (ischaemic condition) over the first fifty to seventy stimulations provides a measure of the contractile ATP cost per twitch (ATP/twitch hereafter) under the respective conditions. The estimated ATP/twitch under aerobic stimulation is not different from that measured under ischaemic stimulation for either muscle (Table 3). A lower ATP/twitch and faster recovery rate in ankle dorsiflexors as compared with the wrist flexor muscles is also apparent in Table 3. The combination of reduced contractile cost and higher oxidative capacity is consistent with the 3-fold difference in stimulation rate needed to achieve the same changes in metabolite levels in the two muscles (Fig. 3).

Glycolytic flux

The third step in our analysis involved quantifying the fate of the end-products of glycolysis to determine glycolytic flux. In general, it is a difficult task to quantify separately the fate of pyruvate via pyruvate dehydrogenase and carboxylase, by transamination to alanine or by reduction to lactate (Jucker *et al.* 1997). We used a simplified approach with assumptions justified in the Methods and Discussion to extract the predominant fluxes from the ^{31}P spectra alone. We measured the fate of glycolytic end-products as either proton production (measured as storage and consumption, eqn (5)) or pyruvate oxidation (eqn (6)) as shown in Fig. 5. This flux is expressed as PCr synthesis since phosphorylation is linked to carbon flux in glycolysis. In both muscles, the flux appearing as proton production was less under aerobic than ischaemic conditions. We assumed that half the oxidized substrate was pyruvate, as has been found in human muscle *in vivo* at low exercise levels (see Brooks & Mercier, 1994). This proportion of glycolytic flux consumed

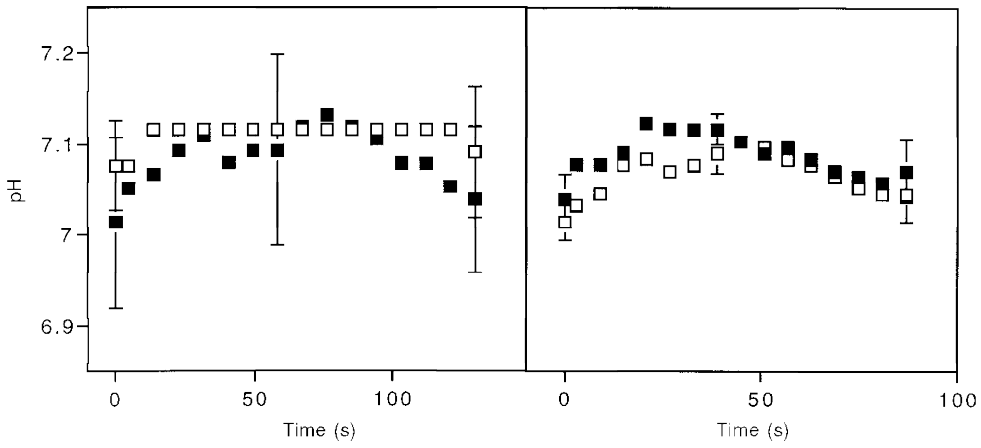

Figure 4. Muscle pH as a function of time during the aerobic (■) and ischaemic (□) stimulation periods

Time starts at the onset of stimulation, for wrist flexors (left panel) and ankle dorsiflexors (right panel). Values are means and the bars are the S.E.M. Sample sizes are 7 subjects for the wrist flexors and 6 subjects for the ankle dorsiflexors.

Table 3. Contractile cost per twitch during stimulation and the PCr recovery rate constant after stimulation

Muscle	Condition	Contractile cost per twitch (mM twitch^{-1})	Initial oxidative phosphorylation rate (mM s^{-1})	Recovery rate constant (s^{-1})
Wrist flexors	Aerobic	0·138 (0·013)	0·128 (0·017)	0·016 (0·0023)
	Ischaemic	0·143 (0·011)	0·267 (0·027)	0·019 (0·0015)
Ankle dorsiflexors	Aerobic	0·107 (0·014)	0·210 (0·027)	0·026 (0·005)
	Ischaemic	0·094 (0·014)	0·423 (0·026)	0·026 (0·0025)

Values are means (± S.E.M.).

by oxidation generates about a quarter of the PCr synthesis found under ischaemic conditions (Fig. 5).

Ischaemic *vs.* aerobic stimulation. We used the sum of H^+ production and pyruvate oxidation to compare flux under the two treatments. Figure 6 shows that total glycolytic PCr synthesis was similar under aerobic and ischaemic conditions. Starting from the delayed onset of glycolytic PCr synthesis (50–70 stimulations), flux increased linearly with the number of stimulations to similar extents by the end of the stimulation period under the two treatments. Despite a small shortfall in glycolytic PCr synthesis under aerobic conditions that was apparent at the last two to three data points, the similarity of flux under the two conditions indicates that total substrate flux and PCr generation by glycolysis is similar under aerobic and ischaemic conditions.

The next result was that glycolytic flux primarily depends on the stimulation number but not on the concentration of P_i. The linear change in glycolytic PCr synthesis through the exercise period under both conditions indicates that glycolytic flux is proportional to stimulation number independent of the presence of oxygen (Fig. 6). In contrast, Fig. 7 shows that PCr synthesis as a function of $[P_i]$ differs strikingly between ischaemic and aerobic conditions in both muscles. Since [ADP] also differs nearly 2-fold between these conditions (Table 2), while glycolytic flux remains the same, there is no clear relationship between the putative feedback regulators of glycolysis, $[P_i]$ and [ADP], and glycolytic PCr synthesis.

DISCUSSION

Lactate generation by muscle during exercise has been attributed to intracellular hypoxia (see Gladden, 1996). The assumption has been that flux of substrates in glycolysis in excess of that oxidized by the mitochondria must reflect an oxygen limitation to oxidative phosphorylation. Our results demonstrate that H^+ generation (and therefore lactate production) under aerobic conditions does not reflect tissue hypoxia, but rather is a result of independent control of

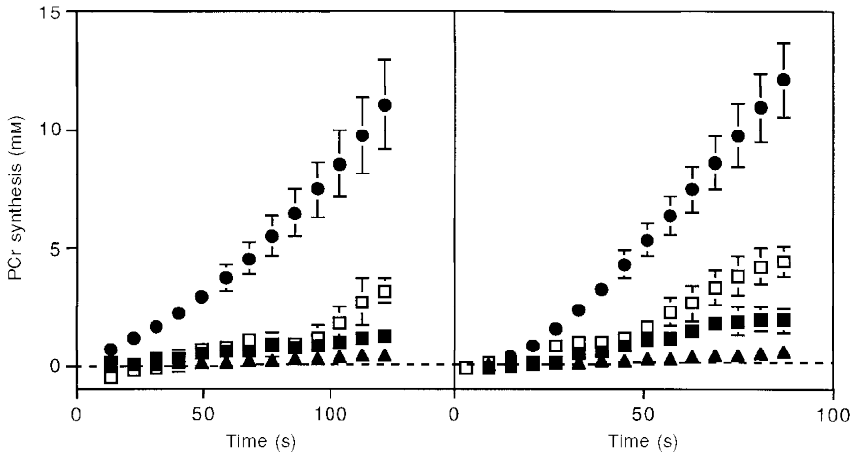

Figure 5. Partitioning of the extent of PCr synthesis as a function of time during the aerobic (filled symbols) and ischaemic (open symbols) stimulation periods

Oxidative phosphorylation (eqn (2), ●); proton generation (eqn (5); aerobic (■) and ischaemic (□) stimulation) for wrist flexors (left panel) and ankle dorsiflexors (right panel); and glycolytic flux that is oxidized under aerobic conditions (eqn (6), ▲) assuming 50% of the substrate used by oxidative phosphorylation is pyruvate. Values, bars and sample sizes as in Fig. 4.

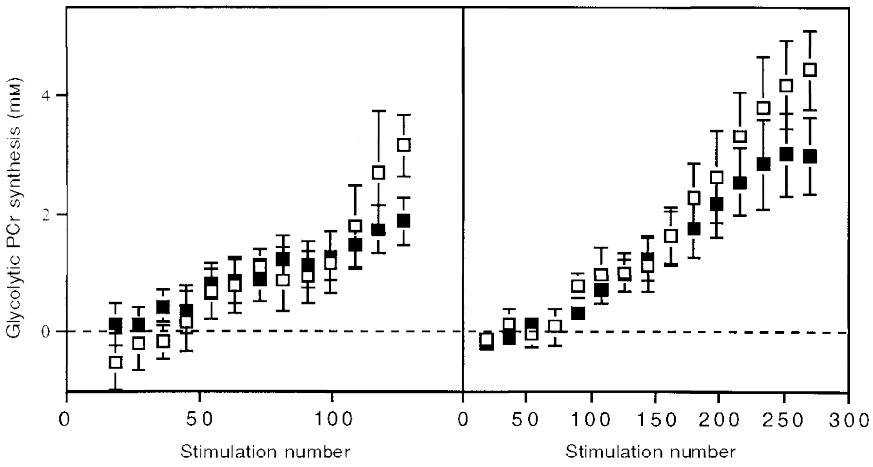

Figure 6. The extent of glycolytic PCr synthesis as a function of the number of stimulations during aerobic (■) and ischaemic (□) stimulation periods

Wrist flexors, left panel; ankle dorsiflexors, right panel. Values, bars and sample sizes as in Fig. 4.

glycolysis and of oxidative phosphorylation. Recently, we have shown that glycolytic flux varies with muscle stimulation rate under ischaemic conditions *in vivo* in the human wrist flexor muscles (Conley *et al.* 1997). Elevated $[Ca^{2+}]$ results from stimulation and is a known regulator of glycogenolysis (Connett & Sahlin, 1996) that may also regulate key enzymes in glycolysis (Luther & Lee, 1986; Parra & Pette, 1995). Such a mechanism would regulate glycolysis in proportion to the ATP demand of contraction independent of feedback by metabolites, oxidative phosphorylation or the presence of O_2. The experiments reported here compare glycolytic flux under aerobic and ischaemic conditions to determine if muscle stimulation provides the signal governing glycolytic flux in the presence of O_2 as it does under ischaemia.

Quantifying oxidative phosphorylation

A major limitation to evaluating glycolytic control during exercise has been quantifying glycolytic flux under aerobic conditions. We have shown how the ^{31}P spectrum can be used to quantify proton generation by glycolysis *in vivo* in muscle under ischaemic conditions (Conley *et al.* 1997). The key to quantifying glycolysis under aerobic conditions is determining the fraction of pyruvate flux that is not reduced to lactate but rather is consumed in oxidative phosphorylation. Figure 1 shows how we used the recovery of PCr after exercise to estimate the oxidative phosphorylation rate during exercise. Only oxidative phosphorylation generates ATP during this recovery because there is no detectable glycolysis in the absence of muscle stimulation even though $[P_i]$ and [ADP] are high (Wilkie *et*

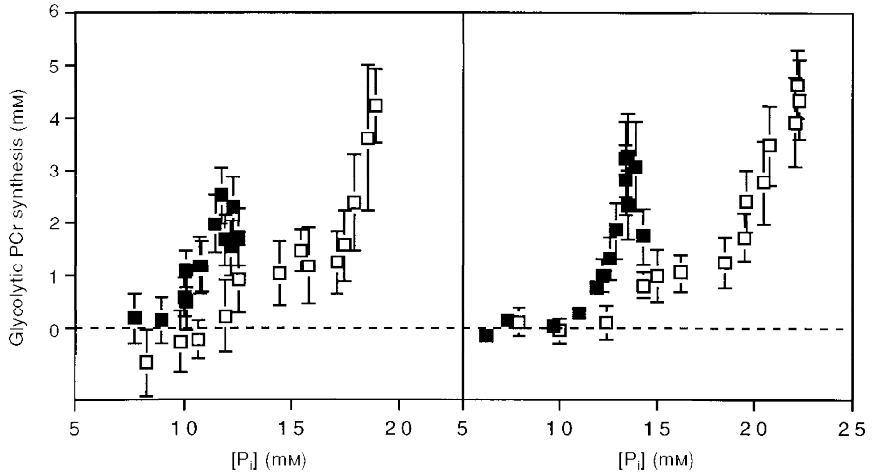

Figure 7. Glycolytic PCr synthesis as a function of $[P_i]$ during the aerobic (■) and ischaemic (□) stimulations

Wrist flexors, left panel; ankle dorsiflexors, right panel. Values, bars and sample sizes as in Fig. 4.

al. 1984; Quistorff *et al.* 1992; Blei *et al.* 1993). Thus the relationship between [ADP] and phosphorylation rate ($\Delta PCr_a/\Delta t$) in Fig. 1*B* can be used to estimate the oxidative synthesis of PCr at each time point throughout stimulation (Fig. 1*C*).

Metabolic changes with exercise

The role of oxidative phosphorylation in PCr synthesis during muscle stimulation is apparent in the nearly 2-fold differences in PCr depletion between ischaemic and aerobic exercise for the two muscles (Fig. 3). The higher [PCr] under aerobic stimulation reflects the large contribution of oxidative phosphorylation during the first minutes of muscle exercise. Subtraction of this oxidative PCr synthesis permits estimation of the contractile costs under aerobic stimulation (Fig. 1*D*), which does not significantly differ from those measured under ischaemic conditions (Table 3). This agreement confirms that oxidative phosphorylation is the major source of PCr synthesis during the initial stimulation period prior to the onset of glycolysis. The similarity in contractile cost confirms that muscle activation did not change under ischaemic *vs.* aerobic conditions in support of our previous finding that the compound muscle action potential is unchanged under these conditions (Blei *et al.* 1993).

Quantifying glycolysis

The ability to characterize oxidative phosphorylation during stimulation offers a means of quantifying the pyruvate flux that is oxidized. Our method does not distinguish between pyruvate metabolism by pyruvate dehydrogenase or carboxylation to oxaloacetate (see Jucker *et al.* 1997), but estimates the total flux into oxidative phosphorylation. In addition, alanine formation from pyruvate is included in our H^+ accounting because both lactate and alanine are fully dissociated weak acids. The fate of pyruvate that is not oxidized is reduction to lactate and the generation of H^+, which is quantified by measurements of the metabolite and pH changes during stimulation. We started with the glycolytic flux that generates H^+, which can be directly quantified with our approach. Protons are either consumed in the creatine kinase reaction when PCr is broken down or accumulate in the muscle (as reflected by a decrease in muscle pH). The large difference in PCr depletion between the two treatments shown in Fig. 3 means much higher consumption of protons under ischaemic stimulation, while little difference is apparent in the pH dynamics under the two conditions (Fig. 4). The difference in H^+ consumption in the creatine kinase reaction therefore largely accounts for the higher H^+ production under ischaemic as compared with aerobic conditions (Fig. 5). The result is that less glycolytic flux ends up as H^+ and lactate under aerobic conditions than under ischaemia during the latter half of the stimulation period.

An additional fate for the end-products of glycolysis is pyruvate oxidation, and the resultant glycolytic PCr synthesis comprises about a quarter of the glycolytic flux found under ischaemia. This estimate of the glycolytic flux consumed by oxidation requires knowledge of the substrate for glycolysis and oxidation, the ATP yield of glycolysis and the rate of oxidative phosphorylation. Glycolysis supplies 50–100 % of the substrate oxidized in untrained humans depending on the level of exercise (Romijn *et al.* 1993; Brooks & Mercier, 1994). We used a conservative estimate that pyruvate comprises 50 % of the substrate for oxidative phosphorylation. Intracellular glycogen provides > 85 % of glycolytic flux in humans and animals during exercise (Romijn *et al.* 1993). Thus, we estimate the glycolytic flux consumed by oxidation based on three ATP molecules generated by glycolysis of glycogen for each thirty-seven ATP molecules generated by oxidative phosphorylation. The relationship with ADP level illustrated in Fig. 1 provides the oxidative phosphorylation rate at each time increment through stimulation. This calculation reveals that a small proportion of glycolytic flux is oxidized and that the predominant product of glycolysis under aerobic conditions in this experiment is H^+ (and lactate). Among the functions for this apparently excessive flux is the need for transamination to alanine in branched chain amino acid oxidation (Jucker *et al.* 1997), maintenance of NADH reduction state in the cytosol (Connett, 1988), and direct ATP supply to ion pumps (James *et al.* 1996).

Control of glycolysis

Comparison of glycolytic PCr synthesis under ischaemic and aerobic stimulation provides a test of the control mechanism governing glycolysis. Figure 6 shows that the glycolytic flux under aerobic conditions is very similar as a function of stimulation rate to that under ischaemic conditions. The shortfall in our measurement of glycolytic flux at the latter time points under aerobic relative to ischaemic stimulation could be due to two uncertainties in our analysis: (1) H^+ efflux from muscle or (2) pyruvate oxidation greater than 50 % of oxidative phosphorylation. The alkalinization of pH and return to control levels by the end of stimulation under both conditions eliminates significant net H^+ efflux during the aerobic stimulation experiment. However, underestimation of pyruvate oxidation is a likely possibility for two reasons. First, this experiment activates all muscle fibres during stimulation and therefore involves the most glycolytic fibres that are normally recruited only at high voluntary exercise intensities. Recruitment of these highly glycolytic fibres is associated with a high glycolytic flux and pyruvate comprises nearly 100 % of the substrate for oxidative phosphorylation under this condition (see Connett & Sahlin, 1996). Second, a high glycolytic flux inhibits fatty acid oxidation, thereby favouring pyruvate oxidation (Coyle *et al.* 1997). Assuming that oxidative phosphorylation oxidizes only pyruvate results in the glycolytic PCr synthesis superimposing under the two conditions (not shown). Thus, the oxidized fraction of glycolysis may approach the near-complete reliance on pyruvate oxidation seen in exercise at the aerobic limit (see Brooks & Mercier, 1994).

We can distinguish between a feedforward (open-loop) control by a factor related to muscle stimulation and metabolic feedback (closed-loop) by [P_i] or [ADP] because we used identical stimulation rates to generate different metabolite levels under the two conditions (Fig. 3). A similar increase in glycolytic PCr synthesis with stimulation number is apparent for both the wrist flexors and ankle dorsiflexors under the two conditions (Fig. 6). In contrast, very different fluxes as a function of [P_i] are apparent under aerobic as compared with ischaemic conditions in both muscles (Fig. 7). Kemp *et al.* (1994) have reported similar differences in glycolytic flux *vs.* [P_i] between ischaemic and aerobic exercise in human forearm muscle. Clearly, glycolytic flux is varying with stimulation number and not with [P_i]. Since [ADP] differs under the two conditions as did [P_i] (Table 2), glycolytic control by metabolite feedback can be eliminated as a quantitatively important mechanism for regulating glycolysis during these types of exercise.

These results confirm the contention that glycolytic flux is proportional to a factor related to muscle stimulation such as Ca^{2+} (Danforth & Helmreich, 1964; Karpatkin *et al.* 1964; Özand & Narahara, 1964; Wilkie *et al.* 1984; Quistorff *et al.* 1992; Conley *et al.* 1997). Calcium activation of phosphorylase *a* is an established mechanism by which muscle stimulation triggers a cascade of events that regulates glycogenolysis. The reversible phosphorylation of phosphorylase *a* that results from this signalling cascade activates this enzyme for the phosphorolysis of glycogen. Our previous finding (Conley *et al.* 1997) that glycogenolytic flux was greater than glycolytic flux during stimulation shows that a mass action effect alone does not account for the increased glycolytic flux. Instead, the difference in fluxes that we measured provides evidence in intact human muscle for a separate control of glycogen phosphorolysis from glycolysis. This separate control is evident in the activation of phosphorylase *a* by adrenaline (epinephrine) without a similar increase in glycolytic flux in skeletal muscle (Karpatkin *et al.* 1964; Chesley *et al.* 1995). The increase in glycolysis with muscle stimulation appears to involve a reversible phosphorylation of phosphofructokinase (PFK; Özand & Narahara, 1964; Luther & Lee, 1986; Parra & Pette, 1995). This phosphorylation facilitates binding of PFK with F-actin which reduces the K_m for its substrate and increases the K_m for allosteric inhibitors such as ATP (Luther & Lee, 1986). Thus, reversible activation of phosphorylase *a* and PFK by Ca^{2+} resulting in glycogen mobilization and increased glycolytic flux can account for our reported finding of distinct glycogenolytic and glycolytic flux *in vivo* during stimulation in human muscle (Conley *et al.* 1997).

Independent control of glycolysis and oxidative phosphorylation

The control of glycolysis by a factor related to muscle stimulation is an example of feedforward control or open-loop control (Houk, 1988). This type of control contrasts with the feedback regulatory mechanism for oxidative phosphorylation (Chance & Williams, 1956; Jeneson *et al.* 1996). Such independence of control of these two pathways is consistent with the mismatch between the delivery of glycolytic substrates and the demands of oxidative phosphorylation seen in this and other experiments (Connett *et al.* 1984, 1986; Connett & Sahlin, 1996). Lactate generation has been reported to occur in muscle with no evidence of hypoxia based on intracellular oxygen partial pressures well above that required for respiration (Connett *et al.* 1986). The production of lactate by fully aerobic tissue has been termed aerobic glycolysis and found to occur in a wide range of tissues, including skeletal muscle (James *et al.* 1996). The distinct regulation of glycolysis and oxidative phosphorylation is consistent with aerobic glycolysis and provides a mechanism for the generation of lactate in fully aerobic skeletal muscle.

Adams, G. R., Foley, J. M. & Meyer, R. A. (1990). Muscle buffer capacity estimated from pH changes during rest-to-work transition. *Journal of Applied Physiology* **69**, 968–972.

Blei, M. L., Conley, K. E. & Kushmerick, M. J. (1993). Separate measures of ATP utilization and recovery in human skeletal muscle. *Journal of Physiology* **465**, 203–222.

Brooks, G. A. & Mercier, J. (1994). Balance of carbohydrate and lipid utilization during exercise: the 'cross-over' concept. *Journal of Applied Physiology* **76**, 2253–2261.

Chance, B. & Williams, G. R. (1956). The respiratory chain and oxidative phosphorylation. *Advances in Enzymology* **17**, 65–134.

Chesley, A., Hultman, E. & Spriet, L. L. (1995). Effects of epinephrine infusion on muscle glycogenolysis during intense aerobic exercise. *American Journal of Physiology* **268**, E127–134.

Conley, K. E., Blei, M. L., Richards, T. L., Kushmerick, M. J. & Jubrias, S. A. (1997). Activation of glycolysis in human muscle *in vivo*. *American Journal of Physiology* **273**, C306–315.

Connett, R. J. (1988). The cytosolic redox is coupled to VO_2. A working hypothesis. *Advances in Experimental Medicine and Biology* **222**, 133–142.

Connett, R. J., Gayeski, T. E. & Honig, C. R. (1984). Lactate accumulation in fully aerobic, working, dog gracilis muscle. *American Journal of Physiology* **246**, H120–128.

Connett, R. J., Gayeski, T. E. & Honig, C. R. (1986). Lactate efflux is unrelated to intracellular P_{O_2} in a working red muscle *in situ*. *Journal of Applied Physiology* **61**, 402–408.

Connett, R. J. & Sahlin, K. (1996). Control of glycolysis and glycogen metabolism. In *Handbook of Physiology. Exercise: Regulation and Integration of Multiple Systems*, ed. Rowell, L. & Shepherd, J., pp. 870–911. Oxford University Press, New York.

Coyle, E. F., Jeukendrup, A. E., Wagenmakers, A. J. M. & Saris, W. H. M. (1997). Fatty acid oxidation is directly regulated by carbohydrate metabolism during exercise. *American Journal of Physiology* **273**, E268–275.

Danforth, W. H. & Helmreich, E. (1964). Regulation of glycolysis in muscle I. The conversion of phosphorylase *b* to phosphorylase *a* in frog sartorius muscle. *Journal of Biological Chemistry* **239**, 3133–3138.

Gladden, L. B. (1996). Lactate transport and exchange during exercise. In *Handbook of Physiology. Exercise: Regulation and Integration of Multiple Systems*, ed. Rowell, L. & Shepherd, J., pp. 614–648. Oxford University Press, New York.

Harris, R., Hultman, E. & Nordesjo, L.-O. (1974). Glycogen, glycolytic intermediates and high-energy phosphates determined in biopsy samples of musculus quadriceps femoris of man at rest. Methods and variance of values. *Scandinavian Journal of Clinical Laboratory Investigation* **33**, 109–120.

Houk, J. (1988). Control strategies in physiological systems. *FASEB Journal* **2**, 97–107.

James, J. H., Fang, C.-H., Schrantz, S. J., Hasselgren, P.-O., Paul, R. J. & Fischer, J. E. (1996). Linkage of aerobic glycolysis to sodium–potassium transport in rat skeletal muscle. *Journal of Clinical Investigation* **98**, 2388–2397.

Jeneson, J. A. L., Wiseman, R. W., Westerhoff, H. V. & Kushmerick, M. J. (1996). The signal transduction function for oxidative phosphorylation is at least second order in ADP. *Journal of Biological Chemistry* **271**, 27995–27998.

Johnson, M., Polgar, J., Weightman, D. & Appleton, D. (1973). Data on the distribution of fibre types in thirty-six human muscles: an autopsy study. *Journal of the Neurological Sciences* **18**, 111–129.

Jucker, B. M., Rennings, A. J. M., Cline, G. W., Petersen, K. F. & Shulman, G. I. (1997). *In vivo* NMR investigation of intramuscular glucose metabolism in conscious rats. *American Journal of Physiology* **273**, E139–148.

Karpatkin, S., Helmreich, E. & Cori, C. F. (1964). Regulation of glycolysis in muscle II. Effect of stimulation and epinephrine in isolated frog sartorius muscle. *Journal of Biological Chemistry* **239**, 3139–3145.

Kemp, G. J., Thompson, C. H., Barnes, P. R. J. & Radda, G. K. (1994). Comparisons of ATP turnover in human muscle during ischaemic and aerobic exercise using ^{31}P magnetic resonance spectroscopy. *Magnetic Resonance in Medicine* **31**, 248–258.

Kushmerick, M. J. (1997). Multiple equilibria of H^+, K^+, Mg^{2+} with ATP, PCr, ADP and P_i in muscle bioenergetics. *American Journal of Physiology* **272**, C1739–1747.

Kushmerick, M. J. & Meyer, R. A. (1985). Chemical changes in rat leg muscle by phosphorus nuclear magnetic resonance. *American Journal of Physiology* **248**, C542–549.

Lawson, J. W. & Veech, R. L. (1979). Effects of pH and free Mg^{2+} on the K_{eq} of the creatine kinases reaction and other phosphate hydrolyses and phosphate transfer reactions. *Journal of Biological Chemistry* **254**, 6528–6537.

Luther, M. A. & Lee, J. C. (1986). The role of phosphorylation in the interaction of rabbit muscle phosphofructokinase with F-actin. *Journal of Biological Chemistry* **261**, 1753–1759.

Özand, P. & Narahara, H. T. (1964). Regulation of glycolysis in muscle III. Influence of insulin, epinephrine, and contraction on phosphofructokinase activity in frog skeletal muscle. *Journal of Biological Chemistry* **239**, 3146–3152.

Parra, J. & Pette, D. (1995). Effects of low-frequency stimulation on soluble and structure-bound activities of hexokinase and phosphofructokinase in rat fast-twitch muscle. *Biochimica et Biophysica Acta* **1251**, 154–160.

Quistorff, B., Johansen, L. & Sahlin, K. (1992). Absence of phosphocreatine resynthesis in human calf muscle during ischaemic recovery. *Biochemical Journal* **291**, 681–686.

Romijn, J. A., Coyle, E. F., Sidossis, L. S., Gastaldelli, A., Horowitz, J. F., Endert, E. & Wolfe, R. R. (1993). Regulation of endogenous fat and carbohydrate metabolism in relation to exercise intensity and duration. *American Journal of Physiology* **265**, E380–391.

Wilkie, D. R., Dawson, M. J., Edwards, R. H. T., Gordon, R. E. & Shaw, D. (1984). ^{31}P NMR studies of resting muscle in normal human subjects. *Advances in Experimental Medicine and Biology*, **170**, 333–348.

Yamada, T., Kikuchi, K. & Sugi, H. (1993). ^{31}P nuclear magnetic resonance studies on the glycogenolysis regulation in resting and contracting skeletal muscle. *Journal of Physiology* **460**, 273–286.

Acknowledgements

We thank the following for their contributions to this study: Drs M. Elaine Cress, Peter Esselman and Ib Odderson. This work was supported by grants from the US NIH (AG-10853, AR-41928) and NSF (IBN-9306596).

Corresponding author

K. E. Conley: Department of Radiology, Box 357115, University of Washington Medical Center, Seattle, WA 98195-7115, USA.

Email: kconley@u.washington.edu